International Journal of Control, Automation and Systems 18(2) (2020) 339-350
http://dx.doi.org/10.1007/s12555-019-0184-4
ISSN:1598-6446 eISSN:2005-4092
http://www.springer.com/12555

Double Closed-loop Integral Terminal Sliding Mode for a Class of Underactuated Systems Based on Sliding Mode Observer

Wei Liu, Si-yi Chen*, and Hui-xian Huang

Abstract: Aiming to solve the tracking control problem of a class of second-order underactuated mechanical systems with unknown model parts, external disturbances and noise disturbances, a double closed-loop layered integral terminal sliding mode control method based on sliding mode observer is proposed. At the outset, the Lagrange model of the system is transformed into an affine model, and a sliding mode observer is designed according to the system structure. Neatly, the outer loop controller is designed using the observer's estimated state, and the output value of the outer loop controller is filtered with a low pass filter. Then the inner loop controller is designed by using hierarchical sliding mode control method. On a premise of ensuring tracking performance, the control method can maximally improve convergence speed and reduce chattering even if there are unknown model parts, external interference and noise interference phenomena in the system. This simulation results distinctly display the effectiveness of the control tactics.

Keywords: Observer, sliding mode control, stability analysis, underactuated system.

1. INTRODUCTION

In recent years, the public pays more and more attention to the improvement of underactuated systems. It usually appears in mechanical systems where the actuator is less than the control degree of freedom. It is widely applied in space robots [1, 2], underwater robots [3, 4], structural flexible robots [5], bridge cranes [6] and other practical systems, and many papers on underactuated system control have been published [7–9]. In a nutshell, controller design and stability analysis of nonlinear underactuated dynamic systems have always been an important research field.

Sliding mode control is a special kind of nonlinear discontinuous control [10–13]. Because the sliding mode can be designed and is independent of the object parameters and disturbances, the sliding mode control has the advantages of fast response, insensitive to the corresponding parameter changes and disturbances, no on-line identification of the system and simple physical realization. It provides an effective way for robust design of time-delay systems [14–16], uncertain systems [17, 18] and underactuated systems [19, 20]. In recent years, the simplicity of sliding mode control for second-order systems in laboratory has attracted extensive attention of researchers. An adaptive hyper-torsional decoupling terminal sliding mode control technique is proposed for a class of fourth-order systems in reference [21]. An adaptive global terminal sliding mode control scheme for tracking control of uncertain nonlinear systems is proposed in reference [22]. a generalized terminal sliding surface is proposed for second-order systems in reference [23]. The second-order dynamic sliding mode control for non-minimum phase underactuated hypersonic vehicle is proposed in [24]. However, some state knowledge of complex underactuated systems is actually difficult to satisfy, because these state variables are not always physically meaningful, and sometimes their measurements are complex or even technically impossible. In addition, in order to reduce the cost and maintenance, it is usually necessary to design state observers to provide real-time estimation of state vectors to reduce the use of sensors. Such as, a hierarchical sliding mode control method for a class of second order underactuated systems based on sliding mode observer is proposed in [25]. However, the designed sliding mode observer has chattering phenomena [26], and the anti-noise ability of the system is not analyzed.

In this paper, a double closed-loop integral terminal sliding mode control strategy based on observer is proposed for second-order underactuated systems. The contributions of this paper are as follows:

1) An improved sliding mode observer is proposed for a class of second order underactuated systems, and its stability is proved by Lyapunov stability theorem.

Manuscript received March 18, 2019; revised July 13, 2019; accepted July 18, 2019. Recommended by Associate Editor Niket Kaisare under the direction of Editor Jessie (Ju H.) Park.

Wei Liu, Si-yi Chen, and Hui-xian Huang are with School of information engineering, Xiangtan University, Xiangtan 411105, P. R. China (e-mails: 601312957@qq.com, c.siyi@xtu.edu.cn, 1062396679@qq.com).
* Corresponding author.

2) An integral terminal sliding mode control strategy with inner and outer loops is designed for the state estimation signal of the observer. The low-pass filter is used to filter the output signal of the outer loop. The stability of the system and the controller is proved by Lyapunov stability principle and Barbalat theory.

3) The simulation results of inverted pendulum verify the robustness and effectiveness of the proposed method.

The rest of this paper is organized as follows: A class of underactuated systems is formulated in Section 2. Design of an improved sliding mode observer for second order underactuated systems is shown in Section 3. A double closed-loop integral terminal sliding mode controller based on observer estimation state is designed and its stability is proved in Section 4. The inverted pendulum model is simulated in Section 5. Finally, some conclusions are given in Section 6.

2. PROBLEM DESCRIPTION

Considering a 2-DOF underactuated system, according to Lagrange equation, the system can be expressed as:

$$\boldsymbol{M}(\boldsymbol{q})\ddot{\boldsymbol{q}}+\boldsymbol{C}(\boldsymbol{q},\dot{\boldsymbol{q}})\dot{\boldsymbol{q}}+\boldsymbol{G}(\dot{\boldsymbol{q}})=\boldsymbol{T}, \tag{1}$$

where $\boldsymbol{q}=[q_1,q_2]^{\mathrm{T}}$, $\boldsymbol{M}(\boldsymbol{q})=\begin{bmatrix} m_{11}(\boldsymbol{q}) & m_{12}(\boldsymbol{q}) \\ m_{21}(\boldsymbol{q}) & m_{22}(\boldsymbol{q}) \end{bmatrix}$, $\boldsymbol{C}(\boldsymbol{q},\dot{\boldsymbol{q}})=\begin{bmatrix} c_{11}(\boldsymbol{q},\dot{\boldsymbol{q}}) & c_{12}(\boldsymbol{q},\dot{\boldsymbol{q}}) \\ c_{21}(\boldsymbol{q},\dot{\boldsymbol{q}}) & c_{22}(\boldsymbol{q},\dot{\boldsymbol{q}}) \end{bmatrix}$, $\boldsymbol{G}(\boldsymbol{q})=\begin{bmatrix} q_1(\boldsymbol{q}) \\ g_2(\boldsymbol{q}) \end{bmatrix}$. If $\boldsymbol{T}=[0,\ u]^{\mathrm{T}}$, it is a type I system. If $\boldsymbol{T}=[u,\ 0]^{\mathrm{T}}$, it is type II system [27].

In order to design the controller conveniently, equation (1) is transformed into affine form. Let $x_1=q_1$, $x_2=\dot{q}_1$, $x_3=q_2$, $x_4=\dot{q}_2$, the dynamic model becomes:

$$\begin{cases} \dot{x}_1(t)=x_2(t), \\ \dot{x}_2(t)=f_1(x,t)+b_1(x,t)u(t)+d_1(x,t), \\ \dot{x}_3(t)=x_4(t), \\ \dot{x}_4(t)=f_2(x,t)+b_2(x,t)u(t)+d_2(x,t), \end{cases} \tag{2}$$

where $\boldsymbol{x}=[x_1,\ x_2,\ x_3,\ x_4]'$ is the system state variable. $f_1(\boldsymbol{x},t)$, $b(\boldsymbol{x},t)$, $f_2(\boldsymbol{x},t)$ and $b_2(\boldsymbol{x},t)$ are nonlinear function. $u(t)$ is the control input signal. $d_1(\boldsymbol{x},t)$ and $d_2(\boldsymbol{x},t)$ denote the system parameter uncertainty and external interference respectively.

Assumption 1: $f_1(\boldsymbol{x},t)$, $b_1(\boldsymbol{x},t)$, $f_2(\boldsymbol{x},t)$ and $b_2(\boldsymbol{x},t)$ are nominal bounded nonlinear functions.

Assumption 2: The system in (2) is bounded input bounded output and is stable for $t\in[0,T]$.

Assumption 3: The uncertain terms are bounded by: $|d_1(\boldsymbol{x},t)|\le\delta_1$ and $d_2(\boldsymbol{x},t)\le\delta_2$, where δ_1 and δ_2 are known positive constants.

3. DESIGN OF THE OBSERVER

According to [25] and system (2), the following improved sliding mode observer is designed.

$$\begin{cases} \dot{\hat{x}}_1(t)=\hat{x}_2(t)+(\mu_1+|x_1-\hat{x}_1|)sign(x_1-\hat{x}_1), \\ \dot{\hat{x}}_2(t)=\hat{f}_1(\bar{x},t)+\hat{b}_1(\bar{x},t)u(t) \\ \qquad\quad +(\mu_2+|\bar{x}_2-\hat{x}_2|)sign(\bar{x}_2-\hat{x}_2), \\ \dot{\hat{x}}_3(t)=x_4(t)+(\mu_3+|x_3-\hat{x}_3|)sign(x_3-\hat{x}_3), \\ \dot{\hat{x}}_4(t)=\hat{f}_2(\bar{x},t)+\hat{b}_2(\bar{x},t)u(t) \\ \qquad\quad +(\mu_4+|\bar{x}_4-\hat{x}_4|)sign(\bar{x}_4-\hat{x}_4), \end{cases} \tag{3}$$

where function estimation of $\hat{f}_1(\bar{\boldsymbol{x}},t)$, $\hat{b}_1(\bar{\boldsymbol{x}},t)$, $\hat{f}_2(\bar{\boldsymbol{x}},t)$ and $\hat{b}_2(\bar{\boldsymbol{x}},t)$ for $f_1(\boldsymbol{x},t)$, $b_1(\boldsymbol{x},t)$, $f_2(\boldsymbol{x},t)$ and $b_2(\boldsymbol{x},t)$, respectively. $\bar{\boldsymbol{x}}=[\bar{x}_1,\bar{x}_2,\bar{x}_3,\bar{x}_4]$ is a new state estimation variable in the following form:

$$\begin{cases} \bar{x}_1=x_1, \\ \bar{x}_2=\hat{x}_2+(\mu_1+|x_1-\hat{x}_1|)\tanh\left(\dfrac{\pi}{2}(\bar{x}_1-\hat{x}_1)\right), \\ \bar{x}_3=x_3, \\ \bar{x}_4=\hat{x}_4+(\mu_3+|x_3-\hat{x}_3|)\tanh\left(\dfrac{\pi}{2}(\bar{x}_3-\hat{x}_3)\right). \end{cases} \tag{4}$$

Tanh is a commonly used hyperbolic tangent function with smooth and continuous characteristics, and can be used as a continuous approximation of sign function.

The estimated error of the observer is as follows:

$$e_{1e}=x_1-\hat{x}_1,\ e_{2e}=x_2-\hat{x}_2,\ e_{3e}=x_3-\hat{x}_3,\ e_{4e}=x_4-\hat{x}_4.$$

Theorem 1: Assuming that 1, 2, 3 and any initial conditions exist, it is assumed that the system (2) constructs an observer (3). By choosing the appropriate parameter μ_i ($i=1,\ 2,\ 3,\ 4$) to estimate the system state variables, the estimated system state variables will converge to the actual system state variables in finite time.

Proof: Firstly, we choose positive definite Lyapunov function V_1.

$$V_1=\frac{1}{2}e_{1e}^2+\frac{1}{2}e_{3e}^2. \tag{5}$$

On both sides of (5), the derivative of time t is obtained.

$$\begin{aligned} \dot{V}_1=&e_{1e}\dot{e}_{1e}+e_{3e}\dot{e}_{3e}=e_{1e}(\dot{x}_1-\dot{\hat{x}}_1)+e_{3e}(\dot{x}_3-\dot{\hat{x}}_3) \\ =&e_{1e}\left(e_{2e}-(\mu_1+|x_1-\hat{x}_1|)sign(x_1-\hat{x}_1)\right) \\ &+e_{3e}\left(e_{4e}-(\mu_3+|x_3-\hat{x}_3|)sign(x_3-\hat{x}_3)\right). \end{aligned} \tag{6}$$

We choose

$$\begin{cases} \mu_1+|x_1-\hat{x}_1|>\max|e_{2e}|\to e_{1e} \\ \Rightarrow\mu_1>\max|e_{2e}|-|e_{1e}|\to e_{1e}, \\ \mu_3+|x_3-\hat{x}_3|>\max|e_{4e}|\to e_{3e} \\ \Rightarrow\mu_3>\max|e_{4e}|-|e_{3e}|\to e_{3e} \end{cases} \tag{7}$$

tends toward zero in finite time, and consequently $\dot{e}_{1e}=0$, $\dot{e}_{3e}=0$, which implies that:

$$\begin{cases} e_{2e}=(\mu_1+|x_1-\hat{x}_1|)sign(x_1-\hat{x}_1), \\ e_{4e}=(\mu_3+|x_3-\hat{x}_3|)sign(x_3-\hat{x}_3). \end{cases} \tag{8}$$

So, we can get: $\bar{x}_2=\hat{x}_2|e_{2e}=x_2$, $\bar{x}_4=\hat{x}_4+e_{4e}=x_4$. Then, we choose the positive definite Lyapunov function V_2.

$$V_2=\frac{1}{2}e_{1e}^2+\frac{1}{2}e_{2e}^2+\frac{1}{2}e_{3e}^2+\frac{1}{2}e_{4e}^2. \tag{9}$$

On both sides of (9), the derivative of time t is obtained.

$$\dot{V}_2=e_{1e}\dot{e}_{1e}+e_{2e}\dot{e}_{2e}+e_{3e}\dot{e}_{3e}+e_{4e}\dot{e}_{4e}. \tag{10}$$

And because:

$$\begin{cases} \dot{e}_{1e}=0, \\ \dot{e}_{2e}=-(\mu_2+|\bar{x}_2-\hat{x}_2|)sign(\bar{x}_2-\hat{x}_2)+d_1(\boldsymbol{x},t), \\ \dot{e}_{3e}=0, \\ \dot{e}_{4e}=-(\mu_4+|\bar{x}_4-\hat{x}_4|)sign(\bar{x}_4-\hat{x}_4)+d_2(\boldsymbol{x},t). \end{cases} \tag{11}$$

In combination (10) and (11), we can get:

$$\begin{aligned} \dot{V}_2=&e_{2e}\dot{e}_{2e}+e_{4e}\dot{e}_{4e} \\ =&e_{2e}\left(-(\mu_2+|\bar{x}_2-\hat{x}_2|)sign(\bar{x}_2-\hat{x}_2)+d_1(\boldsymbol{x},t)\right) \\ &+e_{4e}\left(-(\mu_4+|\bar{x}_4-\hat{x}_4|)sign(\bar{x}_4-\hat{x}_4)+d_2(\boldsymbol{x},t)\right) \\ \leq&-(\mu_2+|\bar{x}_2-\hat{x}_2|)\,|e_{2e}|+\delta_1\,|e_{2e}| \\ &-(\mu_4+|\bar{x}_4-\hat{x}_4|)\,|e_{4e}|+\delta_2\,|e_{4e}|\,. \end{aligned} \tag{12}$$

Therefore, in order to ensure $\dot{V}_2<0$, we can only choose $\mu_2>\delta_1-|\bar{x}_2-\hat{x}_2|$ and $\mu_2>\delta_2-|\bar{x}_4-\hat{x}_4|$. □

Remark 1: Compared with the observer in [25], under the premise of ensuring convergence speed, the improved observer has a larger attraction area even if there is disturbance in the system. A smaller parameter μ_i ($i=1, 2, 3, 4$) can be selected to estimate the state variables of the system to reduce chattering.

4. CONTROL DESIGN

The design of the controller and the observer are independent of each other. The control objective of the system is to design a controller, which enables the system to achieve accurate and fast tracking control even if there are unknown models, external disturbances and noise disturbances. In order to achieve the goal, a double closed-loop hierarchical integration terminal sliding mode control scheme based on sliding mode observer is designed. The controller structure is shown in Fig. 1.

Step 1: According to the output of the observer and the given signal, the sliding surface s_1 and s_2 of the outer loop integration terminal are designed.

$$\begin{cases} s_1=e_1+\int\left(\alpha_1 e_1+\beta_1\,|e_1|^{r_1}\,sign(e_1)\right)dt, \\ s_2=e_2+\int\left(\alpha_2 e_2+\beta_2\,|e_2|^{r_2}\,sign(e_2)\right)dt, \end{cases} \tag{13}$$

where α_1, β_1, α_2, β_2, r_1 and r_2 are positive constants. $e_1=x_{d1}-\hat{x}_1$, $\dot{e}_1=\dot{x}_{d1}-\hat{x}_2$, $e_2=x_{d2}-\hat{x}_3$ and $\dot{e}_2=\dot{x}_{d4}-\hat{x}_4$ are dynamic errors. $\boldsymbol{X}_d=(x_{d1},\dot{x}_{d1},x_{d2},\dot{x}_{d2})$ are given signals.

The derivation of (13) yields:

$$\begin{cases} \dot{s}_1=\dot{e}_1+\alpha_1 e_1+\beta_1\,|e_1|^{r_1}\,sign(e_1) \\ \quad=\dot{x}_{d1}-\hat{x}_2+\alpha_1 e_1+\beta_1\,|e_1|^{r_1}\,sign(e_1), \\ \dot{s}_2=\dot{e}_2+\alpha_2 e_2+\beta_2\,|e_2|^{r_2}\,sign(e_2) \\ \quad=\dot{x}_{d2}-\hat{x}_4+\alpha_2 e_2+\beta_2\,|e_2|^{r_2}\,sign(e_2). \end{cases} \tag{14}$$

The output w_1 and w_2 of the outer loop controller are designed as follows:

$$\begin{cases} w_1=\hat{x}_2=\dot{x}_{d1}+\alpha_1 e_1+\beta_1\,|e_1|^{r_1}\,sign(e_1), \\ w_2=\hat{x}_4=\dot{x}_{d2}+\alpha_2 e_2+\beta_2\,|e_2|^{r_2}\,sign(e_2). \end{cases} \tag{15}$$

Step 2: It should be noted that in the design of inner loop controller, differential explosion will occur when $\dot{w}_1$ and $\dot{w}_2$ are calculated. This disadvantage can be overcome by using low-pass filter. σ_1 and σ_2 are the output values of w_1 and w_2 through low-pass filter $1/\tau_1 s+1$ and $1/\tau_2 s+1$,

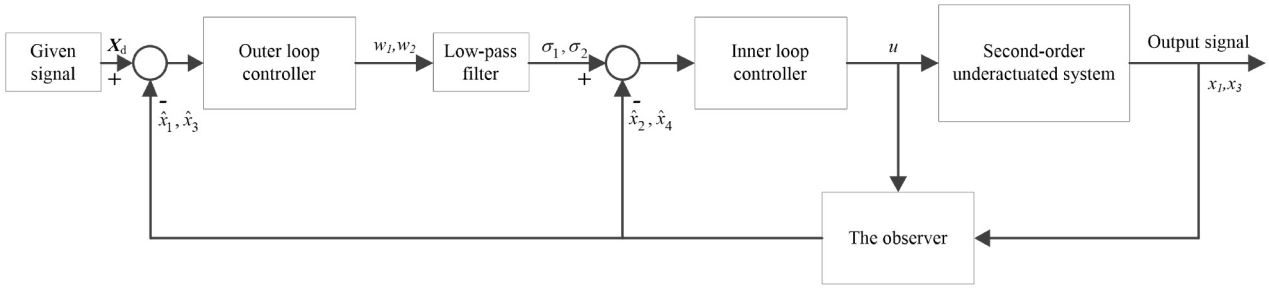

Fig. 1. The controller structure.

respectively, and satisfy the following requirements:

$$\begin{cases} \tau_1\dot{\sigma}_1+\sigma_1=w_1, \\ \sigma_1(0)=w_1(0), \\ \tau_2\dot{\sigma}_2+\sigma_2=w_2, \\ \sigma_2(0)=w_2(0). \end{cases} \tag{16}$$

Further inference from (16) shows that:

$$\begin{cases} \dot{\sigma}_1=\dfrac{w_1-\sigma_1}{\tau_1}, \\ \dot{\sigma}_2=\dfrac{w_2-\sigma_2}{\tau_2}. \end{cases} \tag{17}$$

Therefore, filtering errors y_1 and y_2 can be expressed as:

$$\begin{cases} y_1=\sigma_1-w_1, \\ y_2=\sigma_2-w_2. \end{cases} \tag{18}$$

Lemma 1 [28]**:** $V\in\mathbf{R}$ while $V\geq 0$, the solution to the inequality $\dot{V}\leq -\alpha V+f$ $(\forall t\geq t_0\geq 0)$ is:

$$V(t)\leq e^{-\alpha(t-t_0)}V(t_0)+\int_{t_0}^{t}e^{-\alpha(t-\tau)}f(\tau)d\tau, \tag{19}$$

where α is any constant.

A positive definite Lyapunov function V_3 is defined as follows:

$$V_3=\frac{1}{2}e_1^2+\frac{1}{2}e_2^2+\frac{1}{2}y_1^2+\frac{1}{2}y_2^2. \tag{20}$$

Theorem 2: Assuming that conditions 1, 2, 3 and any initial conditions exist, assuming that the output of the outer loop controller are w_1 and w_2, and the output of the low pass filter are σ_1 and σ_2, and selecting $V_3(0)\leq p$ and $p>0$, all signals of the outer loop controller and the low pass filter are bounded and convergent.

Proof: We define K_1 and K_2 as the following equations:

$$\begin{aligned} K_1&=-\dot{w}_1=-\ddot{x}_{d1}-\alpha_1\dot{e}_1-\beta_1 r_1|e_1|^{r_1-1}\dot{e}_1 sign(e_1) \\ &=-\alpha_1(\dot{x}_{d1}-\sigma_1+y_1)-\ddot{x}_{d1}-\beta_1 r_1|e_1|^{r_1-1}\dot{e}_1 sign(e_1), \\ K_2&=-\dot{w}_2=-\ddot{x}_{d2}-\alpha_2\dot{e}_2-\beta_2 r_2|e_2|^{r_2-1}\dot{e}_2 sign(e_2) \\ &=-\alpha_2(\dot{x}_{d2}-\sigma_2+y_2)-\ddot{x}_{d2}-\beta_2 r_2|e_2|^{r_2-1}\dot{e}_2 sign(e_2). \end{aligned} \tag{21}$$

When $V_3=\frac{1}{2}e_1^2+\frac{1}{2}e_2^2+\frac{1}{2}y_1^2+\frac{1}{2}y_2^2=p$, then K_1 and K_2 are bounded, denoted as $N_1\leq|K_1|$, $N_2\leq|K_2|$.

The derivative of V_3 can be obtained as follows:

$$\begin{aligned} \dot{V}_3=&e_1(\dot{x}_{d1}-\dot{x}_{d1}-\alpha_1 e_1-\beta_1|e_1|^{r_1}sign(e_1)) \\ &+e_2(\dot{x}_{d2}-\dot{x}_{d2}-\alpha_2 e_2-\beta_2|e_2|^{r_2}sign(e_2)) \\ &+y_1(\frac{-y_1}{\tau_1}+K_1)+y_2(\frac{-y_2}{\tau_2}+K_2) \\ =&-\alpha_1 e_1^2-\beta_1|e_1|^{r_1+1}-\alpha_2 e_2^2-\beta_2|e_2|^{r_2+1}-\frac{1}{\tau_1}y_1^2 \\ &-\frac{1}{\tau_2}y_2^2+y_1K_1+y_2K_2 \\ \leq&-\alpha_1 e_1^2-\beta_1|e_1|^{r_1+1}-\alpha_2 e_2^2-\beta_2|e_2|^{r_2+1}-\frac{1}{\tau_1}y_1^2 \\ &-\frac{1}{\tau_2}y_2^2+|y_1||K_1|+|y_2||K_2| \\ \leq&-\alpha_1 e_1^2-\beta_1|e_1|^{r_1+1}-\alpha_2 e_2^2-\beta_2|e_2|^{r_2+1}-\frac{1}{\tau_1}y_1^2 \\ &-\frac{1}{\tau_2}y_2^2+\frac{1}{2}\left((|y_1||K_1|)^2+1\right)+\frac{1}{2}\left((|y_2||K_2|)^2+1\right) \\ =&-\alpha_1 e_1^2-\alpha_2 e_2^2+\left(\frac{1}{2}K_1^2-\frac{1}{\tau_1}\right)y_1^2 \\ &+\left(\frac{1}{2}K_2^2-\frac{1}{\tau_2}\right)y_2^2-\beta_1|e_1|^{r_1+1}-\beta_2|e_2|^{r_2+1}+1. \end{aligned} \tag{22}$$

If we choose $\alpha_1\geq r$, $\alpha_2\geq r$, $1/\tau_1\geq 0.5N_1^2+r$, $1/\tau_2\geq 0.5N_2^2+r$ and $r>0$, and because $N_1\leq|K_1|$, $N_2\leq|K_2|$, $\beta_1>0$ and $\beta_2>0$. Then there are:

$$\begin{aligned} \dot{V}_3\leq&-re_1^2-re_2^2+\left(\frac{1}{2}K_1^2-\frac{1}{2}N_1^2-r\right)y_1^2 \\ &+\left(\frac{1}{2}K_2^2-\frac{1}{2}N_2^2-r\right)y_2^2-\beta_1|e_1|^{r_1+1}-\beta_2|e_2|^{r_2+1} \\ &+1 \\ =&-2rV_3+\frac{1}{2}\left(K_1^2-N_1^2\right)y_1^2+\frac{1}{2}\left(K_2^2-N_2^2\right)y_2^2 \\ &-\beta_1|e_1|^{r_1+1}-\beta_2|e_2|^{r_2+1}+1 \\ \leq&-2rV_3+1. \end{aligned} \tag{23}$$

Since $V_3=p$, (23) can be written as $\dot{V}_3\leq -2rp+1$. To ensure $\dot{V}_3\leq 0$, we can select $-2rp+1\leq 0$, or $r\geq 1/2p$.

At the same time, (1) shows that when $r\geq 1/2p$, $\dot{V}_3\leq 0$, that is, if $V_3(0)\leq p$, V_3 is also in the compact set, and for any time t satisfies $V_3(t)\leq p$, that is, all signals of outer loop controller and low pass filter are bounded.

In addition, the following convergence analysis can be carried out through the above reasoning.

According to Lemma 1, the solution of inequality equation $\dot{V}_3\leq -2rV_3+1$ is

$$\begin{aligned} V_3(t)\leq&e^{-2r(t-t_0)}V(t_0)+\int_{t_0}^{t}e^{-2r(t-\tau)}d\tau \\ =&e^{-2r(t-t_0)}V(t_0)+\frac{1}{2r}(1-e^{-2r(t-t_0)}). \end{aligned} \tag{24}$$

According to (1), we can get $\lim\limits_{t\to\infty}V_3(t)\leq 1/2r$. Therefore, $V_3(t)$ asymptotically converges, and the convergence accuracy depends on r.

Thus, Theorem 2 has been proved. □

Step 3: According to the estimated value of the observer and the output value of the filter, the first level integral terminal sliding surface s_3 and s_4 of the inner loop

controller are designed.

$$\begin{cases} s_3 = e_3 + \int (\alpha_3 e_3 + \beta_3 |e_3|^{r_3} sign(e_3))\, dt, \\ s_4 = e_4 + \int (\alpha_4 e_4 + \beta_4 |e_4|^{r_4} sign(e_4))\, dt, \end{cases} \tag{25}$$

where α_3, β_3, α_4, β_4, r_3 and r_4 are positive constants. $e_3 = \sigma_1 - \hat{x}_2$, $\dot{e}_3 = \dot{\sigma}_1 - \dot{\hat{x}}_2$, $e_4 = \sigma_2 - \hat{x}_4$ and $\dot{e}_4 = \dot{\sigma}_2 - \dot{\hat{x}}_4$ are dynamic errors.

For sliding surface s_3 and s_4, the first derivative of time t is obtained.

$$\begin{cases} \dot{s}_3 = \dot{e}_3 + \alpha_3 e_3 + \beta_3 |e_3|^{r_3} sign(e_3), \\ \dot{s}_4 = \dot{e}_4 + \alpha_4 e_4 + \beta_4 |e_4|^{r_4} sign(e_4). \end{cases} \tag{26}$$

If the first derivatives of sliding surface s_3 and s_4 are equal to zero, the equivalent control law of the inner loop controller can be obtained as follows:

$$\begin{cases} u_{eq1} = \dfrac{1}{\hat{b}_1(\hat{x},t)}\big(-\hat{f}_1(\hat{x},t) + \dot{\sigma}_1 + \alpha_3 e_3 \\ \qquad + \beta_3 |e_3|^{r_3} sign(e_3)\big), \\ u_{eq2} = \dfrac{1}{\hat{b}_2(\hat{x},t)}\big(-\hat{f}_2(\hat{x},t) + \dot{\sigma}_2 + \alpha_4 e_4 \\ \qquad + \beta_4 |e_4|^{r_4} sign(e_4)\big). \end{cases} \tag{27}$$

Second level sliding surface s is defined as follows:

$$s = a_1 s_3 + a_2 s_4, \tag{28}$$

where a_1 and a_2 are positive constants.

The control law of the inner loop controller is designed as follows:

$$u = u_{eq1} + u_{eq2} + u_{sw}. \tag{29}$$

Define positive definite Lyapunov function V_4.

$$V_4 = \frac{1}{2} s^2. \tag{30}$$

To ensure $\dot{V}_4 \le 0$, the switching control law is designed as follows:

$$\begin{aligned} u_{sw} =& \frac{-1}{a_1 \hat{b}_1(\hat{x},t) + a_2 \hat{b}_2(\hat{x},t)} \\ & \times \begin{pmatrix} a_1 \hat{b}_1(\hat{x},t) u_{eq2} + a_2 \hat{b}_2(\hat{x},t) u_{eq1} \\ -ks - \eta sign(s) \end{pmatrix}, \end{aligned} \tag{31}$$

where k and η are positive constants.

Theorem 3: For the underactuated system given by (2), the sliding surfaces are given as (25) and (28), with the control law defined by (31). The sliding surfaces s, s_3 and s_4 are asymptotically stable.

Proof: The derivative of Lyapunov function V_4 is

$$\begin{aligned} \dot{V}_4 =& s\dot{s} = s(a_1 \dot{s}_3 + a_2 \dot{s}_4) \\ =& s\Big[a_1\big(\dot{\sigma}_1 + \alpha_3 e_3 + \beta_3 |e_3|^{r_3} sign(e_3) - \hat{f}_1 - \hat{b}_1 u - d_1\big) \\ & + a_2\big(\dot{\sigma}_2 + \alpha_4 e_4 + \beta_4 |e_4|^{r_4} sign(e_4) - \hat{f}_2 - \hat{b}_2 u - d_2\big)\Big]. \end{aligned} \tag{32}$$

Combining (31) and (32), we can get

$$\begin{aligned} \dot{V}_4 =& s\,(a_1 d_1 + a_2 d_2 - ks - \eta sign(s)) \\ \le& (a_1 d_1 + a_2 d_2)\,|s| - ks^2 - \eta\,|s|\,. \end{aligned} \tag{33}$$

When $\delta = sup(a_1\delta_1 + a_2\delta_2)$ is selected and $\eta > \delta$ is satisfied, there are

$$\dot{V}_4 \le \delta\,|s| - ks^2 - \eta\,|s| = (\delta - \eta)\,|s| - ks^2 \le 0. \tag{34}$$

By calculating the integral of (34), we can get

$$\int_0^t \dot{V}_4 d\tau = \int_0^t \big((\delta - \eta)\,|s| - ks^2\big)\, d\tau. \tag{35}$$

Through further derivation of the above formula, we can get that

$$V_4(t) - V_4(0) = \int_0^t (\delta - \eta)\,|s| - ks^2 d\tau. \tag{36}$$

Because $V_4(t) > 0$, (36) can be changed into

$$\begin{aligned} V_4(0) =& \int_0^t \big((\eta - \delta)\,|s| + ks^2\big)\, d\tau + V_4(t) \\ \ge& \int_0^t \big((\eta - \delta)\,|s| + ks^2\big)\, d\tau. \end{aligned} \tag{37}$$

Therefore, we can get the following results.

$$\lim_{t\to\infty} \int_0^t \big((\eta - \delta)\,|s| + ks^2\big)\, d\tau \le V_4(0) < \infty. \tag{38}$$

So $s^2 \in L_\infty$. Obviously, we can express Barbalat lemma by $\lim_{t\to\infty} s = 0$, and the second level sliding surface s is asymptotically stable.

In addition, we can get

$$\begin{aligned} \int_0^\infty s^2 d\tau =& \int_0^\infty (a_1 s_3 + a_2 s_4)^2 d\tau \\ =& \int_0^\infty (a_1^2 s_3^2 + 2a_1 a_2 s_3 s_4 + a_2^2 s_4^2) d\tau < \infty. \end{aligned} \tag{39}$$

Since $2a_1 a_2 s_3 s_4 \le a_2^2 s_4^2 + a_1^2 s_3^2$ is established, it can be obtained that

$$\int_0^\infty 4a_1 a_2 s_3 s_4 d\tau < \int_0^\infty (a_1 s_3 + a_2 s_4)^2 d\tau < \infty. \tag{40}$$

Therefore, according to (39) and (40), we can get

$$\int_0^\infty s_3^2 d\tau < \infty, \quad \int_0^\infty s_4^2 d\tau < \infty. \tag{41}$$

So $s_3 \in L_\infty$, $s_3^2 \in L_\infty$, $s_4 \in L_\infty$, $s_4^2 \in L_\infty$, obviously, we can use $\lim_{t\to\infty} s_3 = 0$ and $\lim_{t\to\infty} s_4 = 0$ to express Barbalat lemma. Therefore, the sliding surface s_3 and s_4 are asymptotically stable.

Thus, Theorem 3 has been proved. □

5. SIMULATION RESULTS

In order to verify the proposed control method, the cart-pole system was simulated and the proposed method and the methods of [25] is compared. The method in this paper is defined as Case 2, and the method in [25] is defined as Case 1.

The dynamic equation of the cart-pole system can be exhibited in the form of (3) with the functions $f_1(x,t)$, $b_1(x,t_)$, $f_2(x,t)$ and $b_2(x,t)$ as

$$\begin{cases} f_1(x,t) = \dfrac{m_t g \sin(x_1) - m_p L \sin(x_1)\cos(x_1)x_2^2}{L((\frac{4}{3})m_t - m_p \cos^2(x_1))}, \\ b_1(x,t) = \dfrac{\cos(x_1)}{L((\frac{4}{3})m_t - m_p \cos^2(x_1))}, \\ f_2(x,t) = \dfrac{-(\frac{4}{3})m_p L x_2^2 \sin(x_1) + m_p g \sin(x_1)\cos(x_1)}{(\frac{4}{3})m_t - m_p \cos^2(x_1)}, \\ b_2(x,t) = \dfrac{4}{3((\frac{4}{3})m_t - m_p \cos^2(x_1))}, \end{cases} \tag{42}$$

where m_t is the total mass of the cart-pole system which contains the quality of the pole (m_p) and the mass of the cart (m_c), x_1 represents the swing angle of the pole, x_2 expresses the swing speed of the pole, x_3 denotes the position of the cart, x_4 indicates the cart velocity. In these simulations, the parameters are chosen as $m_c = 1$ kg, $m_p = 0.05$ kg, $L = 0.5$ m and $g = 9.8$ m/s^2.

5.1. Without d_1, d_2 and noise

The initial conditions are $\boldsymbol{x}(0) = [-\pi/12,\ 0,\ 0.5,\ 0]^T$, $d_1 = 0$, $d_2 = 0$ and the desired output vector is $y(t) = (0,0)^T$. The parameters of controllers are provided in Table 1.

Table 1. Controller parameters.

Parameters	Case1	Case2
c_1	2.5	-
c_2	0.9	-
$\alpha_1 = \alpha_3 = \alpha_2 = \alpha_4$	-	1.5
$\beta_1 = \beta_3$	-	5
$\beta_2 = \beta_4$	-	1
$r_1 = r_2 = r_3 = r_4$	-	1.2
a_1	1.5	1.5
a_2	1.5	1.5
k	10	10
η	0.05	0.05
$\tau_1 = \tau_2$	-	0.4
μ_i $(i = 1, 2, 3, 4)$	0.5	0.5

Figs. 2-8 represent respectively the trajectories of $\boldsymbol{x}(t)$, their estimators, and their references, the sliding surfaces $s(t)$, $s_3(t)$ and $s_4(t)$, the estimation error of sliding mode observer and the control signal $u(t)$.

It is clear from Figs. 2-5 that the overshoot and adjustment time of Case 2 are less than that of Case 1. As can be seen clearly from Fig. 6, the convergence speed and smoothness of sliding surface of Case 2 are better than that of Case 1. As can be seen from Fig. 7, compared with [25], the proposed sliding mode observer has faster convergence rate of estimation error and no chattering. As can be seen from Fig. 8, the chattering of control input signal of Case 2 is smaller than that of Case 1.

5.2. With d_1, d_2 and noise

The initial conditions are $\boldsymbol{x}(t) = [-ß/12,\ 0,\ -0.2,\ 0]^T$, $d_1 = 0.01\sin(t) + 0.05\sin(x_1)$, $d_2 = 0.01\cos(t) + 0.05\sin(x_3)$, the measured noise is Gauss white noise with

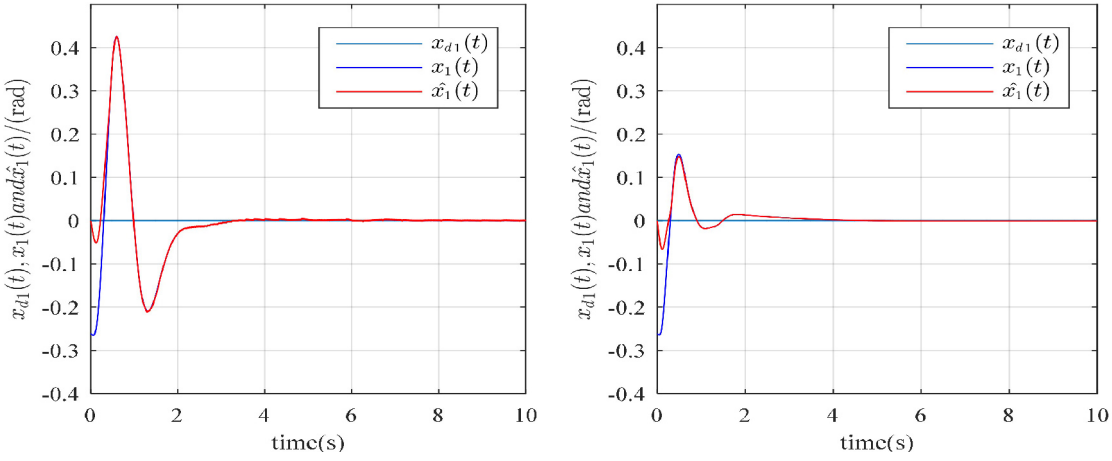

(a) The pole angle of Case 1. (b) The pole angle of Case 2.

Fig. 2. The angle of the pole, its estimation and the reference.

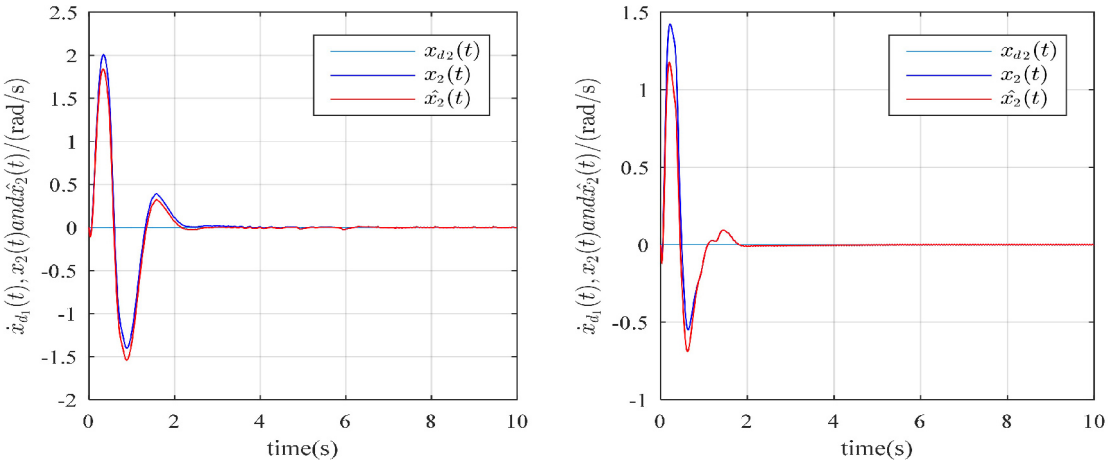

(a) The pole velocity of Case 1. (b) The pole velocity of Case 2.

Fig. 3. The velocity of the pole, its estimation and the reference.

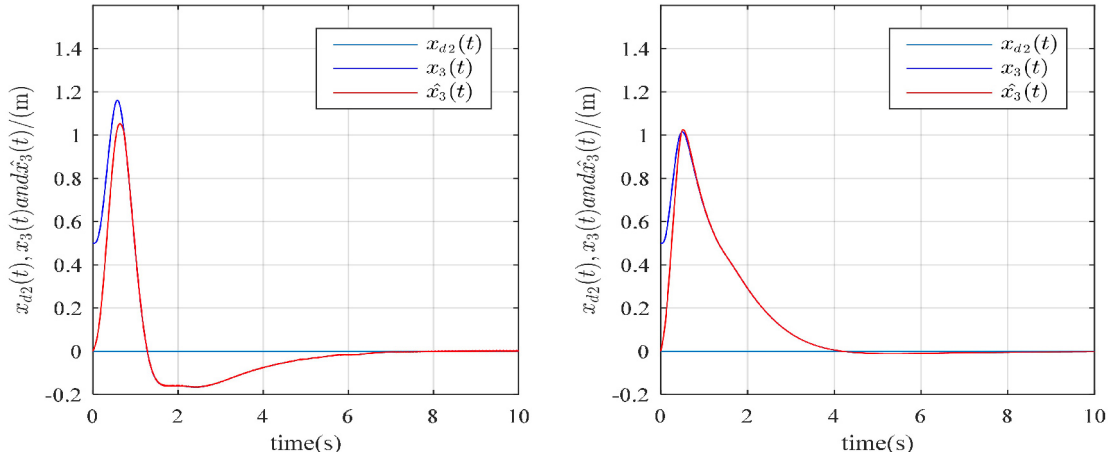

(a) The cart position of Case 1. (b) The cart position of Case 2.

Fig. 4. The position of the cart, its estimation and the reference.

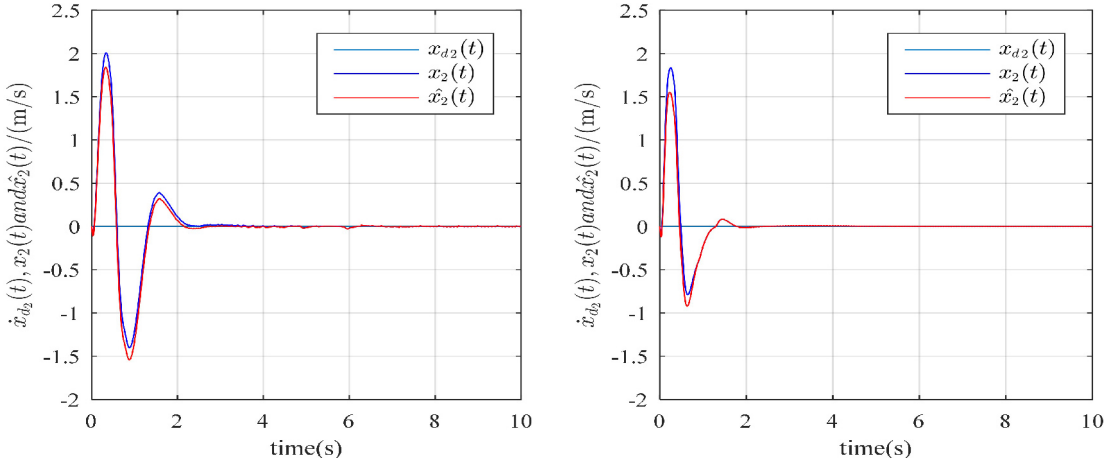

(a) The pole velocity of Case 1. (b) The pole velocity of Case 2.

Fig. 5. The velocity of the cart, its estimation and the reference.

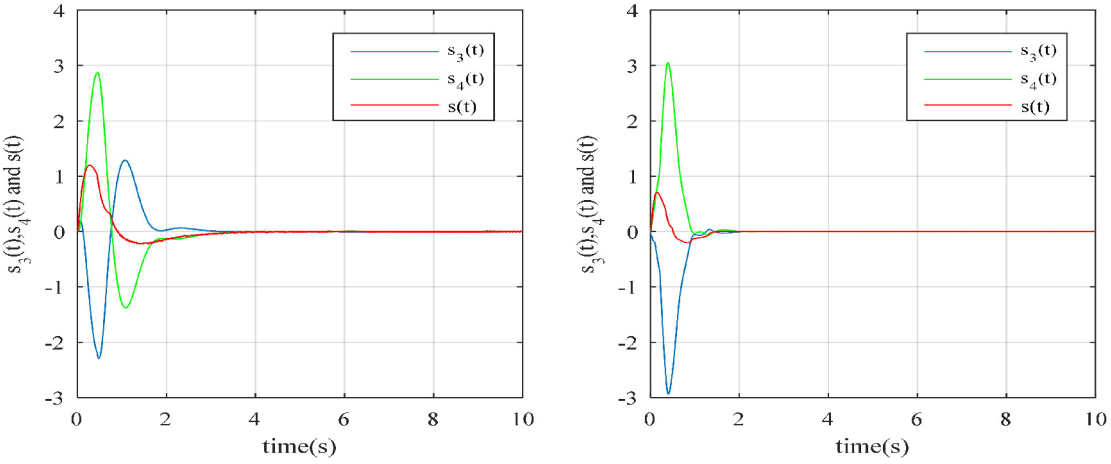

(a) The sliding surfaces of Case 1. (b) The sliding surfaces of Case 2.

Fig. 6. The sliding surfaces $s(t)$, $s_3(t)$ and $s_4(t)$.

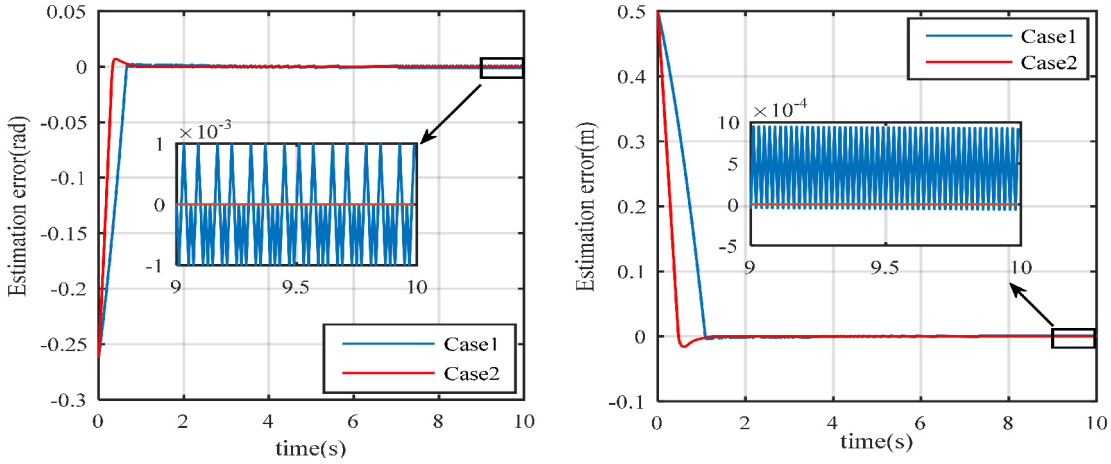

(a) Estimination error of pendulum angle. (b) Estimination error of cart position.

Fig. 7. Estimation error of sliding mode observer.

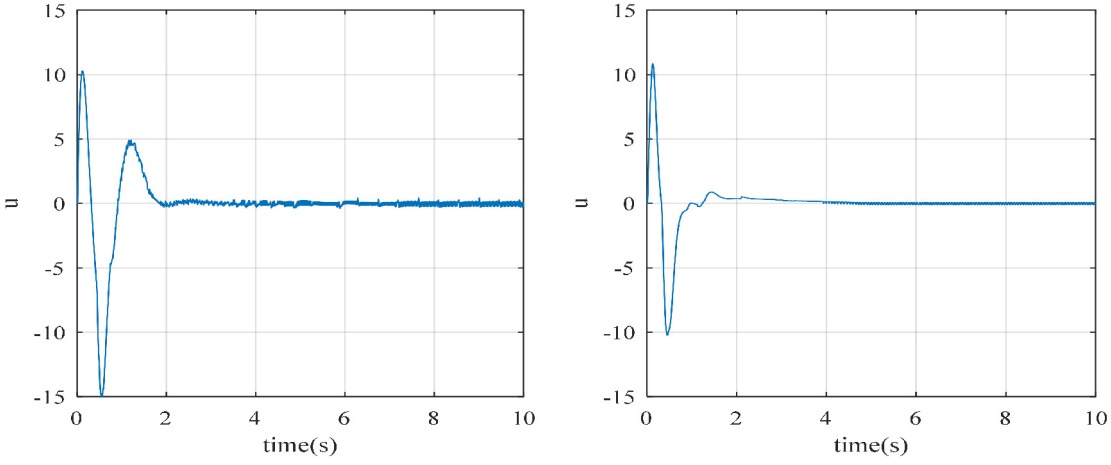

(a) The control signal of Case 1. (b) The control signal of Case 2.

Fig. 8. The control signal $u(t)$.

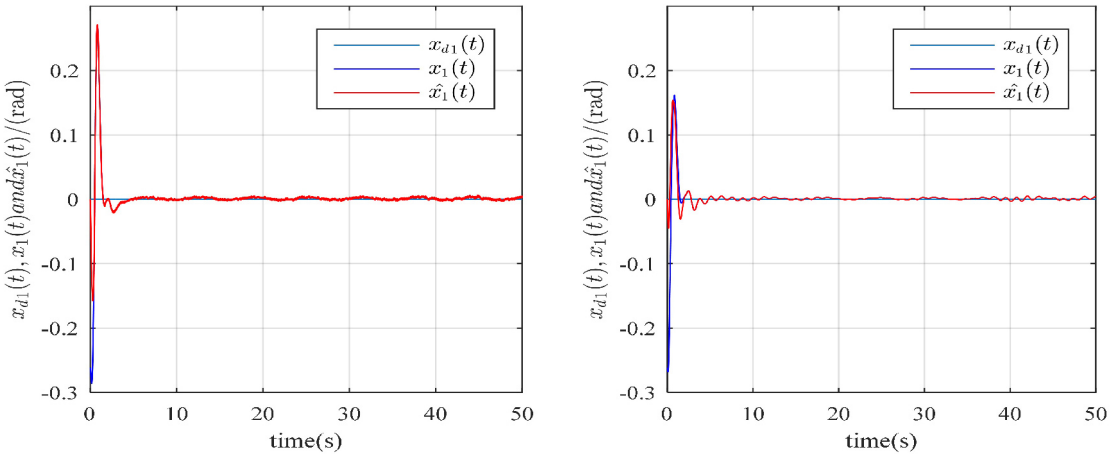

(a) The pole angle of Case 1. (b) The pole angle of Case 2.

Fig. 9. The angle of the pole, its estimination and the reference (with d_1, d_2 and noise).

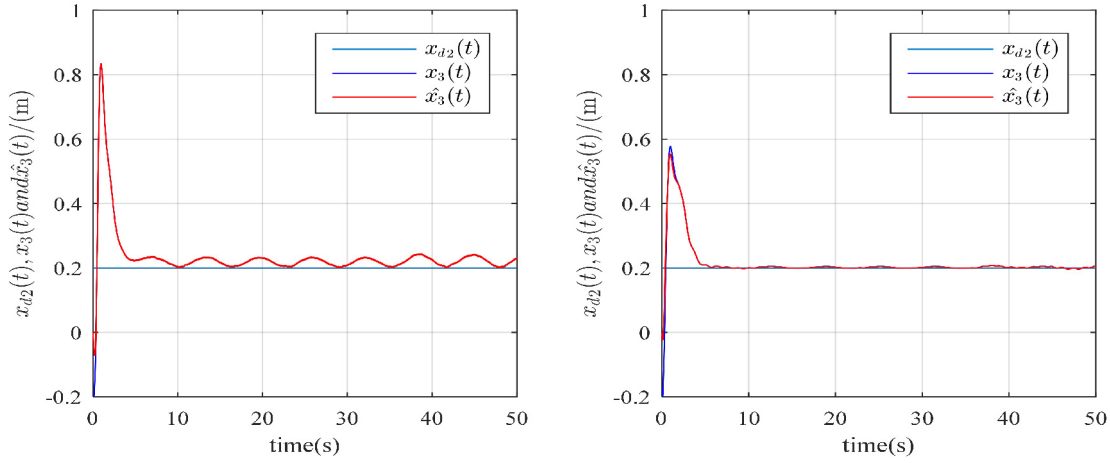

(a) The cart position of Case 1. (b) The cart position of Case 2.

Fig. 10. The position of the cart, its estimation and the reference (with d_1, d_2 and noise).

0.01 amplitude and 0.1 standard deviation, given noise is a random number with an amplitude of 0.001 and the desired output vector is $y(t) = (0, 0.2)^T$. Meanwhile, the parameters of the controller remain unchanged. Measuring noise is added at 20 seconds of simulation time, and then given noise is added at 35 seconds.

Figs. 9-11 represent respectively the trajectories of $x_1(t)$, $x_3(t)$, their estimators, and their references, and the control signal $u(t)$.

From the simulation results of Fig. 9 and Fig. 10, we can clearly see that the pendulum angle and position of Case 1 have obvious oscillation phenomenon, while Case 2 still maintains a good tracking control effect. The control signal in Fig. 11 clearly shows that Case 2 has better noise suppression ability and stronger robustness.

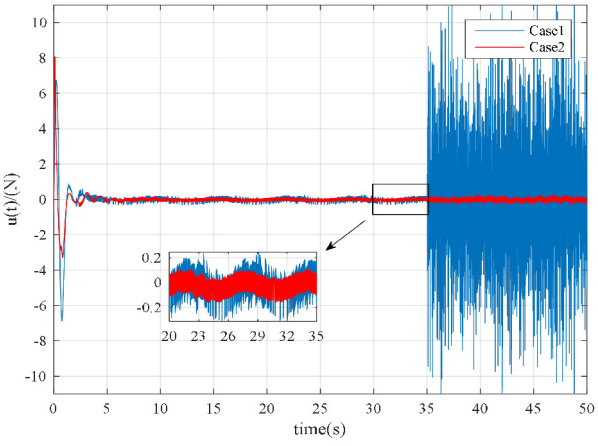

Fig. 11. The control signal $u(t)$ (with d_1, d_2 and noise).

Fig. 12. The practical cart-pole system.

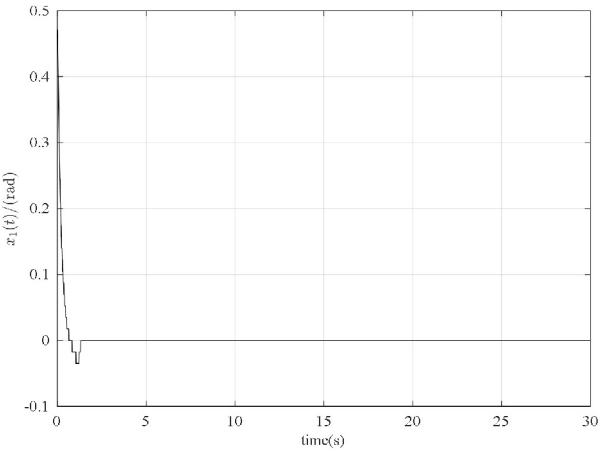

Fig. 13. The angle of the pole.

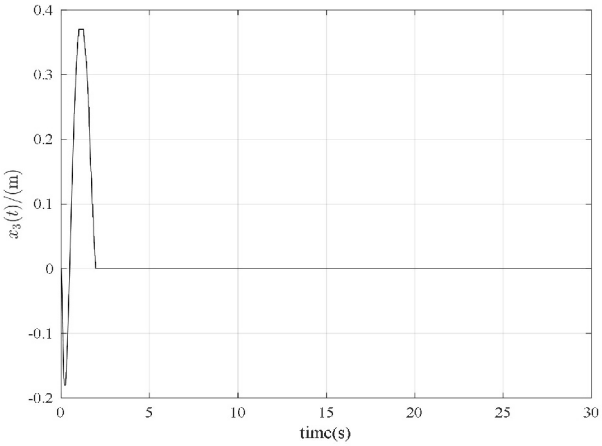

Fig. 14. The position of the cart.

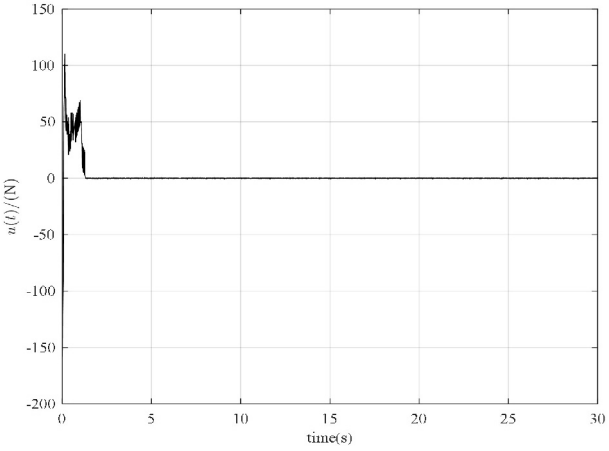

Fig. 15. The control signal $u(t)$.

5.3. Physical simulaton

In this paper, Matlab real-time simulation tool and Simulink toolbox are used to test the designed controller on the actual vehicle system. Fig. 12 shows the linear motor inverted pendulum system manufactured by Hopemotion Co., Ltd. The system is based on the TI TMS320F28335 DSP and MATLAB/Simulink. Simulink can be used to build models, automatically generate code, control and save data and modify parameters online. The initial conditions are $\boldsymbol{x}(0) = [0.47, 0, 0, 0]^T$.

Figs. 13-15 are the experimental curves of the pendulum swing angle, trolley position and control input, respectively. It can be clearly seen that the swing angle, position and control inputs can be maintained at around zero. The results of physical experiments further validate the effectiveness of the scheme.

6. CONCLUSION

In this paper, a double closed-loop hierarchical integral terminal sliding mode control method for a class of underactuated systems is presented. The sliding mode observer is designed by using the affine model of the system. The outer loop controller is designed according to the estimated state. At the same time, low-pass filter is used to filter the output value of the outer loop controller. Then, the inner loop controller is designed by using the hierarchical sliding mode control method. Even if there are unknown model components, external disturbances and noise disturbances in the system, the proposed control method can maximize the convergence speed and reduce chattering. The simulation experiments of the cart inverted pendulum system are carried out without considering the disturbance and the disturbance. The results show the effectiveness and robustness of the control method proposed in this paper. Finally, the effectiveness of the proposed method is further illustrated by the physical simulation experiment of the cart inverted pendulum.

This maneuver method can be used for control of underactuated mechanical systems such as multistage inverted pendulum, mechanical arm system, TORA system and Ball-Plate system [29–34]. It is naturally to draw a conclu-

sion that this application of research to higher-level intelligent control systems is worth keeping to do some further study.

REFERENCES

[1] D. Meng, X. Wang, W. Xu, and B. Liang, "Space robots with flexible appendages: Dynamic modeling, coupling measurement, and vibration suppression," *Journal of Sound and Vibration*, vol. 396, pp. 30-50, 2017.

[2] W. Xu, J. Peng, B. Liang, and Z. Mu, "Hybrid modeling and analysis method for dynamic coupling of space robots," *IEEE Transactions on Aerospace and Electronic Systems*, vol. 52, no. 1, pp. 85-98, February 2016.

[3] J. Bak, H. Nguyen, S. Park, D. Lee, T. Seo, S. Jin, and J. Kim, "Positioning control of an underwater robot with tilting thrusters via decomposition of thrust vector," *International Journal of Control, Automation and Systems*, vol. 15, no. 5, pp. 2283-2291, October 2017.

[4] A. Jonathan, M. Vázquez, H. Rodríguez, V. Vega, and A. Sánchez-Orta, "Fractional sliding mode control of underwater ROVs subject to non-differentiable disturbances," *International Journal of Control, Automation and Systems*, vol. 15, no. 3, pp. 1314-1321, June 2017.

[5] C. Lee, M. Kim, Y. Kim, N. Hong, S. Ryu, H. Kim, and S. Kim, "Soft robot review," *International Journal of Control, Automation and Systems*, vol. 15, no. 1, pp. 3-15, February 2017.

[6] L. Tuan, S. Lee, V. Dang, S. Moon, and B. Kim, "Partial feedback linearization control of a three-dimensional overhead crane," *International Journal of Control, Automation and Systems*, vol. 11, no. 4, pp. 718-727, August 2013.

[7] P. Liu, H. Yu, and S. Cang, "Trajectory synthesis and optimization of an underactuated microrobotic system with dynamic constraints and couplings," *International Journal of Control, Automation and Systems*, vol. 16, no. 5, pp. 2373-2383, October 2018.

[8] R. Rascón, J. Alvarez, and L. Aguilar, "Discontinuous H∞ control of underactuated mechanical systems with friction and backlash," *International Journal of Control, Automation and Systems*, vol. 14, no. 5, pp. 1213-1222, October 2016.

[9] M. Chaalal and N. Achour, "Stabilizing periodic orbits of a class of mechanical systems with impulse effects: a Lyapunov constraint approach," *International Journal of Control, Automation and Systems*, vol. 15, no. 5, pp. 2213-2221, October 2017.

[10] L. Arie, "Sliding order and sliding accuracy in sliding mode control," *International Journal of Control*, vol. 58, no. 6, pp. 17, 1993.

[11] P. G. Grossimon, E. Barbieri, and S. Drakunov, "Sliding mode control of an inverted pendulum," *Proceedings of 28th Southeastern Symposium on System Theory*, Baton Rouge, LA, USA, pp. 248-252, 1996.

[12] H. Huerta, A. G. Loukianov, and J. M. Cañedo, "Passivity sliding mode control of large-scale power systems," *IEEE Transactions on Control Systems Technology*, vol. 27, no. 3, pp. 1219-1227, May 2019.

[13] A. D. Giorgio, A. Giuseppi, F. Liberati, A. Ornatelli, A. Rabezzano, and L. R. Celsi, "On the optimization of energy storage system placement for protecting power transmission grids against dynamic load altering attacks," *Proc. of 25th Mediterranean Conference on Control and Automation (MED)*, Valletta, pp. 986-992, 2017.

[14] H. C Ting, J. L Chang, and Y. P Chen, "Applying output feedback integral sliding mode controller to uncertain time-delay systems with mismatched disturbances," *International Journal of Control, Automation, and Systems*, vol. 9, no. 6, pp. 1056-1066, December 2011.

[15] M. C. Pai, "Observer-based adaptive sliding mode control for nonlinear uncertain state-delayed systems," *International Journal of Control, Automation, and Systems*, vol. 7, no. 4, pp. 536-544, August 2009.

[16] L. R. Celsi, R. Bonghi, S. Monaco, and D. Normand-Cyrot, "On the exact steering of finite sampled nonlinear dynamics with input delays," *IFAC-PapersOnLine*, vol. 48, pp. 674-679, 2015.

[17] J. L. Chang, "Sliding mode control design for mismatched uncertain systems using output feedback," *International Journal of Control, Automation, and Systems*, vol. 14, no. 2, pp. 579-586, April 2016.

[18] L. Xiaofei, Q. Shengbo, R. Malekain, and L. Zhixiong, "Observer-based composite adaptive dynamic terminal sliding-mode controller for nonlinear uncertain SISO systems," *International Journal of Control, Automation, and Systems*, vol. 17, no. 1, pp. 94-106, January 2019.

[19] E. Taha, Z. Mohamed, and K. Youcef-Toumi, "Trajectory tracking sliding mode control of underactuated AUVs," *Nonlinear Dynamics*, vol. 84, no. 2, pp. 1079-1091, April 2016.

[20] A. Nabanita and M. Chitralekha, "Integral backstepping sliding mode control for underactuated systems: swing-up and stabilization of the cart-pendulum system," *ISA Transactions*, vol. 52, no. 6, pp. 870-880, November 2013.

[21] D. A. Haghighi and S. Mobayen, "Design of an adaptive super-twisting decoupled terminal sliding mode control scheme for a class of fourth-order systems," *ISA Transactions*, vol. 75, pp. 216-225, 2018.

[22] S. Mobayen, "Adaptive global terminal sliding mode control scheme with improved dynamic surface for uncertain nonlinear systems," *International Journal of Control, Automation and Systems*, vol. 16, no. 4, pp. 1692-1700, August 2018.

[23] J. Young-Hun, L. Yong-Hwa, and P. Kang-Bak, "Design of generalized terminal sliding mode control for second-order systems," *International Journal of Control, Automation and Systems*, vol. 9, no. 3, pp. 606-610, June 2011.

[24] Z. Wang, W. Bao, and H. Li, "Second order dynamic sliding-mode control for nonminimum phase underactuated hypersonic vehicles," *IEEE Transactions on Industrial Electronics*, vol. 64, no. 4, pp. 3105-3112, April 2017.

[25] D. Zehar, K. Benmahammed, and K. Behih, "Control for underactuated systems using sliding mode observer," *International Journal of Control, Automation and Systems*, vol. 16, no. 2, pp. 739-745, April 2018.

[26] K. Harikumar, T. Bera, R. Bardhan, and S. Sundaram, "Discrete-time sliding mode observer for the state estimation of a manoeuvring target," *Proceedings of the Institution of Mechanical Engineers, Part I: Journal of Systems and Control Engineering*, February 2019.

[27] J. Huang, S. Ri, L. Liu, Y. Wang, J. Kim, and G. Pak, "Nonlinear disturbance observer-based dynamic surface control of mobile wheeled inverted pendulum," *IEEE Transactions on Control Systems Technology*, vol. 23, no. 6, pp. 2400-2407, November 2015.

[28] I. Petros and S. Jing, *Robust Adaptive Control*, Prentice-Hall, Inc, 1995.

[29] M. Rahman, M. Saad, K. Jean-Pierre, and P. Archambault, "Control of an exoskeleton robot arm with sliding mode exponential reaching law," *International Journal of Control, Automation and Systems*, vol. 11, no. 1, pp. 92-104, February 2013.

[30] S. Wang, Z. Wu, and M. Cui, "Tracking controller design for random nonlinear TORA system," *Proc. of Chinese Control and Decision Conference (CCDC)*, Yinchuan, pp. 1836-1840, 2016.

[31] Y. Bao, J. Li, J. Xie, and B. Gao, "On hierarchical sliding mode control of underactuated TORA system," *Proceedings of the 10th World Congress on Intelligent Control and Automation*, Beijing, pp. 1785-1789, 2012.

[32] M. Borah, P. Roy, and B. K Roy, "Enhanced performance in trajectory tracking of a ball and plate system using fractional order controller," *IETE Journal of Research*, vol. 64, no. 1, pp. 76-86, August 2017.

[33] B. Lu, Y. Fang, and N. Sun, "Continuous sliding mode control strategy for a class of nonlinear underactuated systems," *IEEE Transactions on Automatic Control*, vol. 63, no. 10, pp. 3471-3478, October 2018.

[34] C. Hwang, C. Chiang, and Y. Yeh, "Adaptive fuzzy hierarchical sliding-mode control for the trajectory tracking of uncertain underactuated nonlinear dynamic systems," *IEEE Transactions on Fuzzy Systems*, vol. 22, no. 2, pp. 286-299, April 2014.

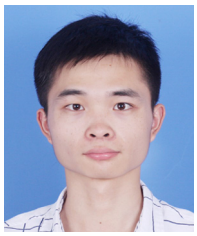

Wei Liu was born in 1994. He is a postgraduate in Xiangtan University. His research interests are theory and application of nonlinear systems.

Si-yi Chen was born in 1986. He is a Ph.D. and a lecturer in Xiangtan University. His research interests are servo control technology, fractional calculus theory and multi-objective optimization theory.

Hui-xian Huang was born in 1957. He is a Ph.D. and a professor in Xiangtan University. His research interests are advanced control theory, process control modeling and application, and power electronics technology.